

## SIMULATION ANALYSIS AND NONDESTRUCTIVE TESTING OF FLEXURAL PERFORMANCE OF WOOD SINGLE LAP GLUED JOINTS

Wei Lu,<sup>a, b</sup> Yingcheng Hu,<sup>a, \*</sup> and Jia Yao<sup>a, b</sup>

The effect of joint size on the loading capacity of wood single lap joints was studied with an orthogonal experimental design. The maximum load, modulus of elasticity, and modulus of rupture were the three mechanical indexes used to evaluate wood joint quality. A simulation model of bending tests was established using the finite element method. The stress distributions of the joints were analyzed; the peak stripping stress was reduced with an increase in gluing length and thickness. The increase in the corresponding experimental values of maximum load was in agreement with this conclusion. The joint force for various loading positions was simulated, and the peak stress was lowest at the location with the maximum offset. Therefore, the bending capacity of the wood joints can be improved by changing the loading position. Nondestructive fast Fourier transform (FFT) testing of the bending vibration was used to obtain the dynamic elastic modulus. A significant correlation existed between modulus of elasticity and modulus of rupture. Finite element simulation analysis and nondestructive testing are all effective methods for quality evaluation of wood joints, and they can be applied to the design and testing of wood joints.

*Keywords:* Single lap joints; Flexural performance; Finite element simulation; Nondestructive testing

*Contact information:* a: Key Laboratory of Bio-based Material Science and Technology of Ministry of Education of China, College of Material Science and Engineering, Northeast Forestry University, Harbin, 150040, China; b: College of Mechanical Engineering, Jiamusi University, 154007, Jiamusi, China.

\*Corresponding author: yingchenghu@163.com

### INTRODUCTION

Laminated veneer lumber (LVL), as a new type of structural material, must meet the requirements of practical use (Li *et al.* 2011). Because of the limits of the production process, veneer must undergo longitudinal lengthening, and veneer joints are inevitably produced. The joints are the weakest links in the LVL structure; therefore, researching joints is of great significance. Under the working conditions of joints, load transmission is mainly realized through the glue line. Thus, the stress distribution within the glued joints is vital for the joint strength. The stripping or peel stress of the glued joint is the most important influential factor, which is generally concentrated in certain areas at both ends of the joint, enabling easier crack failure of the joint ends. However, the gluing properties of wood are seriously affected by its own performance. The strength of wood is usually lower than that of adhesives, so failures usually occur at the interface of the wood and the glue line or within the wood.

Custodio *et al.* (2009) elaborated on the factors influencing durability of glued timber joints. Ye (1989) analyzed the gluing strength of plywood and concluded that the thickness ratio is the most important influence on the stress concentration coefficient.

Researchers have studied the gluing strength and gluing interface, but have largely ignored the problems of stress distribution and stress concentration. In addition, the anisotropic and viscoelastic properties of wood make analysis of the distribution of stress within the glued joints more complex. To date, there has been little published research addressing this topic.

The dispersion of mechanical properties of glue joints is large (Gu 2003), so the reproducibility of measurement indices for destructive joint testing is poor, and the actual strength of the joint is difficult to calculate according to test data. This study adopted both nondestructive testing of the joint performance and finite element simulations (FES) to attempt to avoid this dispersion. Nondestructive testing methods based on FFT technology are relatively mature (Rokhlin and Marom 1986) and extensively reported in the literature (Cohen 1989; Hu 2004; Hu *et al.* 2001; Liu and Ta 2000; Liu *et al.* 2007; Prosser *et al.* 1999; Ta and Liu 2001), but this method has not been used for testing wood joint performance. The FES method has been widely used in the wood composites research (Abdolahian Sohi *et al.* 2011; Yoshihara 2012) and has proved to be very useful. In this study, the FFT bending vibration method was used for flexural performance testing. The aim was to find a new and effective method for the nondestructive testing of wood joints. The structure and size of the joints were the main variables of study. Glue length, width, and thickness were the three factors chosen for the single lap wood glued joints. An orthogonal experiment with these three factors and three levels was designed. Joint performance was evaluated using finite element simulations and FFT bending vibration nondestructive tests, along with destructive bending tests.

## EXPERIMENTAL

### Materials

The birch (*Betula platyphylla* Suk) used for this study was purchased from the Yichun forest region, Heilongjiang, China. Its moisture content was 8%. Polyvinyl acetate emulsion, which can achieve rapid curing at room temperature, was used as an adhesive. The joint type and sample size of the single lap joints are shown in Fig. 1, where  $P$  is the applied load and  $l$ ,  $h$ , and  $b$  are gluing length, sample thickness, and width, respectively.

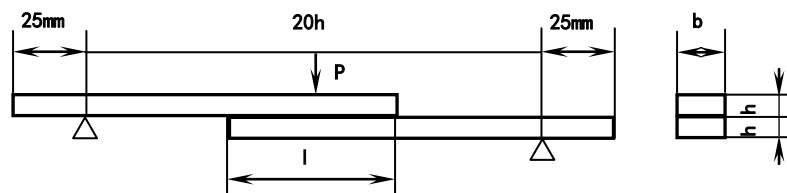


Fig. 1. Single lap joint type and constraint conditions

### Experimental Design

Table 1 shows the factors and levels of the orthogonal experiment studied and the size of the single lap glued joints; each group tested contained five samples. All tests were carried under conditions of constant temperature (about 20 °C) and relative humidity.

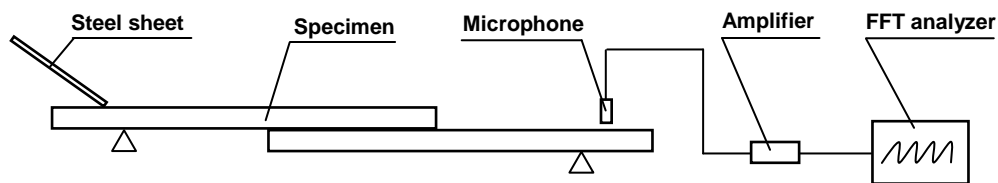
**Table 1.** Factors and Levels of Experiment

Level \ Factors	l (mm)	h (mm)	b (mm)
1	20	5	20
2	40	7	25
3	60	9	30

## Experimental Methods

### *Nondestructive FFT flexural vibration testing*

The flexural vibration method of FFT was performed as shown in Fig. 2. The sample was horizontally supported at the nodes of flexural vibration ( $0.224 L$ , where  $L$  is the total length of sample). A steel sheet, which can induce the sound signal more clearly and can be easily tested by the FFT instrument, was used to knock one side of the sample, and a microphone was used to receive the signal at the other end. The signal was amplified and transmitted to the analyzer to obtain the resonant frequency. Using the TGH (Timoshenko-Goens-Hearmon) method (Cheng and Hu 2011; Hu 2004),  $E_f$  which is the elastic modulus obtained from the nondestructive FFT bending vibration test, was ascertained.

**Fig. 2.** Flexural vibration test method

### *Destructive bending test*

In accordance with the wood-based panel standard GB/T17657-1999 of China and EN 312-1:1997 of Europe, the SANS-CMT5504 universal mechanical testing machine was used to obtain the maximum load ( $P_{max}$ ), modulus of rupture (MOR), and modulus of elasticity (MOE) values (as shown in Table 3) by using three-point destructive bending testing.

## RESULTS AND ANALYSIS

### Results Analysis of Destructive Bending Test

The optimal structural design can be obtained by the intuitive analysis (Cheng 2005) of MOE and MOR, as shown in Table 2. Through a comparison of the factors with extreme difference, the relative importance of each factor can be determined for each mechanical index. Through comprehensive analysis, the order of the impact of each factor on MOE and MOR was  $l > h > b$  and  $h > l > b$ . The optimum schemes were  $l_3h_1b_3$  and  $h_1l_3b_3$ , respectively.

The optimum scheme was chosen as  $l_3h_1b_3$  after comprehensive consideration. The values of MOE and MOR increased with the increase of  $l$ , but were reduced with the increase of  $h$ . The extreme difference of  $b$  was relatively small, so the sample width had a very small impact on MOE and MOR, and the effect can be ignored.

**Table 2.** Experimental Results and Intuitive Analysis

No.	Factors			Average values		
	l (mm)	h (mm)	b (mm)	MOE (GPa)	MOR (MPa)	P <sub>max</sub> (N)
1	20	5	20	17.43	103.05	303.50
2	20	7	25	13.30	73.20	398.52
3	20	9	30	13.01	46.20	486.22
4	40	5	25	28.03	147.52	409.70
5	40	7	30	22.49	115.32	677.38
6	40	9	20	17.81	83.06	503.96
7	60	5	30	38.85	190.50	635.10
8	60	7	20	30.20	125.50	546.66
9	60	9	25	26.38	101.78	723.08
MOE	x <sub>1</sub>	14.58	28.10	21.81		
	x <sub>2</sub>	22.78	22.00	22.57		
	x <sub>3</sub>	31.81	19.07	24.78		
	Extreme difference	17.23	9.04	2.97		
	Optimum plan	l <sub>3</sub>	h <sub>1</sub>	b <sub>3</sub>		l <sub>3</sub> h <sub>1</sub> b <sub>3</sub>
MOR	x <sub>1</sub>	74.15	147.02	103.87		
	x <sub>2</sub>	115.30	104.67	107.50		
	x <sub>3</sub>	139.26	77.01	117.34		
	Extreme difference	65.11	70.01	13.47		
	Optimum plan	l <sub>3</sub>	h <sub>1</sub>	b <sub>3</sub>		h <sub>1</sub> l <sub>3</sub> b <sub>3</sub>

**Correlation Analysis between Nondestructive and Destructive Tests**

Values of  $E_f$  and MOE for all samples are plotted in Fig. 3 as a function of sample number.

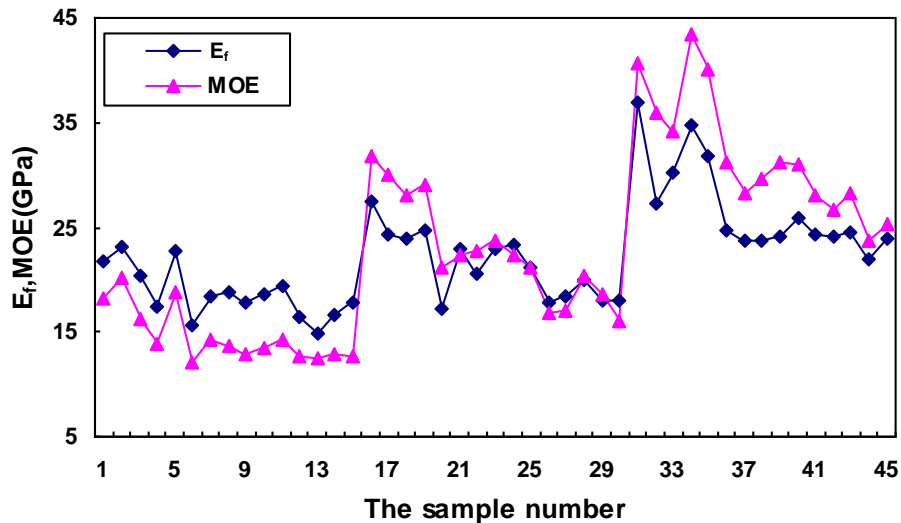


**Fig. 3.**  $E_f$  and MOE for each sample

The values obtained from FFT and destructive tests were not the same, and clear differences could be seen between  $E_f$  and MOE values from the different groups. Because the effect of sample width on MOE can be ignored, the comprehensive effect of  $l$  and  $h$  was considered. It was found that the length to thickness ratio had a significant effect on  $E_f$  and MOE, as shown in Fig. 4. The mean  $E_f$  and MOE generally increased with increasing length to thickness ratio. When the length to thickness ratio was smaller than 5,  $E_f$  was greater than MOE, and vice versa.

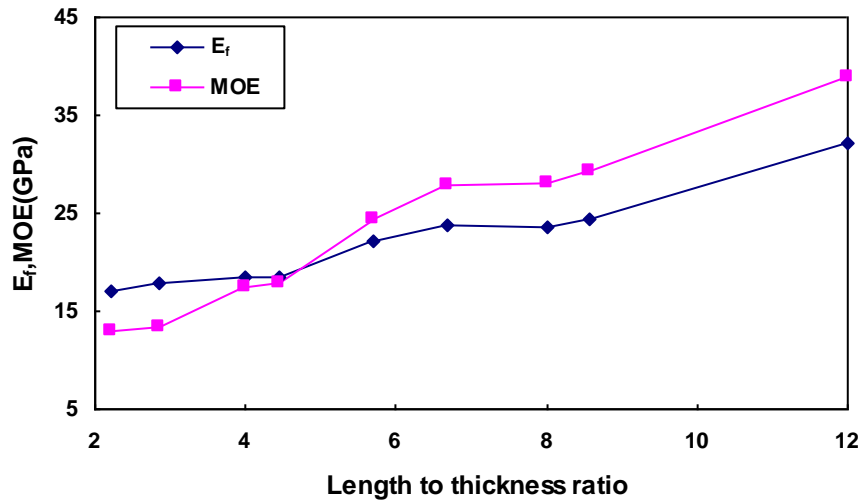


Fig. 4. Relationship between average  $E_f$ , MOE, and length to thickness ratio

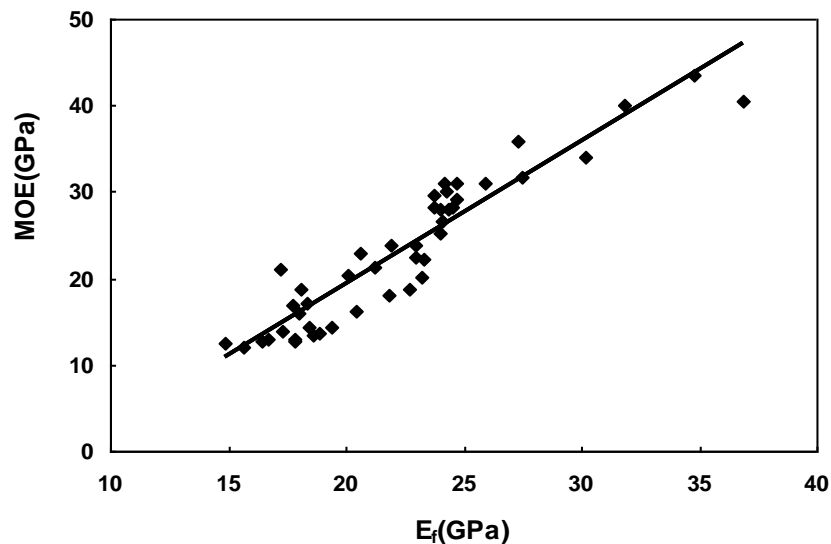


Fig. 5. Regression curve of  $E_f$  and MOE

To determine the correlation between  $E_f$  and MOE or MOR, regression analysis results are shown in Figs. 5 and 6. In Fig. 5, the linear regression equation for  $E_f$  and MOE was  $MOE = 1.6468E_f - 13.643$ . Because the correlation coefficient  $R = 0.9372 > R_{43, 0.001} = 0.4747$ , there was a strong linear correlation between  $E_f$  and MOE; thus the flexural vibration method of FFT can be used to predict MOE by the regression equation. In Fig. 6, the linear regression equation for  $E_f$  and MOR was  $MOR = 7.3524E_f - 54.271$ .

Again, because  $R = 0.8331 > R_{43, 0.001} = 0.4747$ , the regression relationship was also significant, and there was a strong linear correlation between  $E_f$  and MOR.

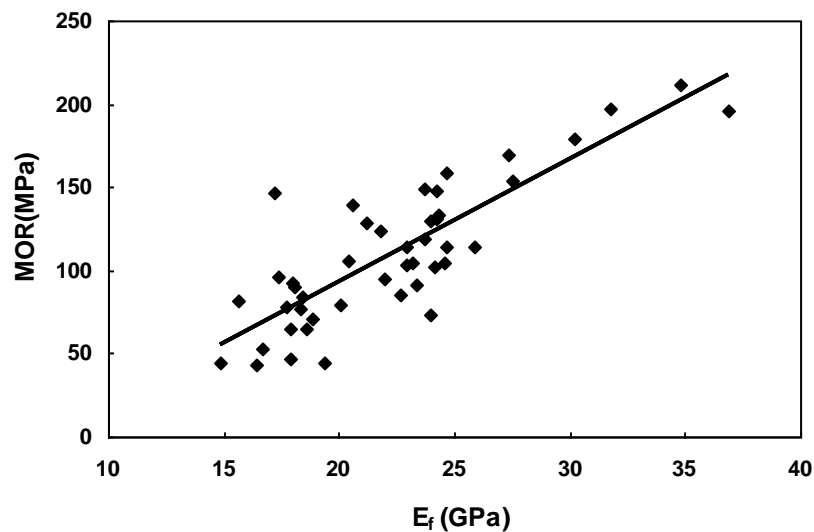


Fig. 6. Regression curve of  $E_f$  and MOR

The above analysis revealed significant correlations between  $E_f$ , MOE, and MOR. Thus, the FFT flexural vibration method can be used for nondestructive testing of wood single lap glue joints and can provide technical support for the quality control of joints.

### Finite Element Simulations

Simulation analysis of the bending performance of birch single lap joints was done using the ANSYS finite element method; the simulation is a linear elastic analysis, and the mesh tool was used to determine the suitable mesh size. The measured physical and mechanical performance of birch is shown in Table 3. The constraints and loading conditions of the model simulation of the bending test are as shown in Fig. 1. The “brick 8 node 45” unit was adopted as the geometric model. A line load “P” was loaded, using a value of 10 MPa.

Table 3. Physical and Mechanical Performance of Birch

Direction	Elastic modulus (MPa)	Poisson ratio	Shear modulus (MPa)
Axial direction	$E_x = 12842$	$\mu_{xy} = 0.524$	$G_{xy} = 996$
Radial direction	$E_y = 1341$	$\mu_{yz} = 0.758$	$G_{yz} = 59$
Tangential	$E_z = 891$	$\mu_{xz} = 0.557$	$G_{xz} = 786$

### Results of Finite Element Simulations

The equivalent von-Mises stress of a sample can be obtained from simulation analysis. As shown in Fig. 7, the stresses were concentrated at joint ends, and the deformations of samples were basically symmetrical. Figure 8 shows the stripping stress distribution curves for the nine group samples (as in Table 2). The peak stripping stress was reduced with increased gluing length, although the change was less at longer lengths. The stress in the middle regions also decreased with increasing gluing length.

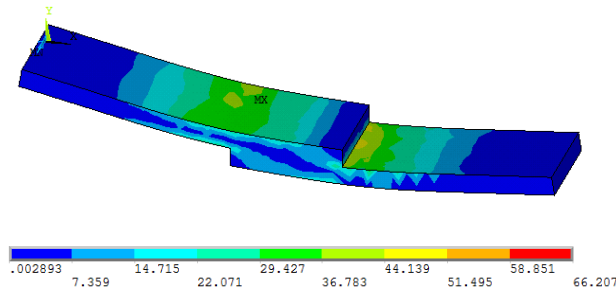


Fig. 7. Equivalent stress graphs of group 4

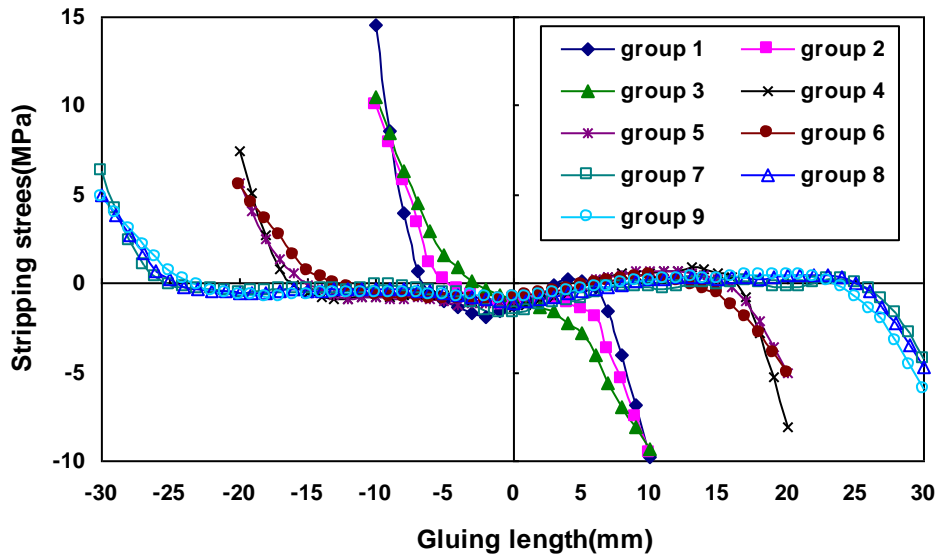


Fig. 8. Stripping stress curves for nine group samples

The peak stripping stress decreased with increasing sample thickness, and the decrease of the peak value corresponded to the increase in the maximum bearing load observed in the destructive bending test (as in Table 2). The trends in the bearing capacity of the joints with changing joint size are reflected in the simulation analyses.

The above simulation analyses show that finite element analysis can be used to simulate the loading positions of joints and analyze the stripping stress distributions that affect the flexural performance. This information can be used to optimize the design of joints in practical applications, in particular the joint bearing position.

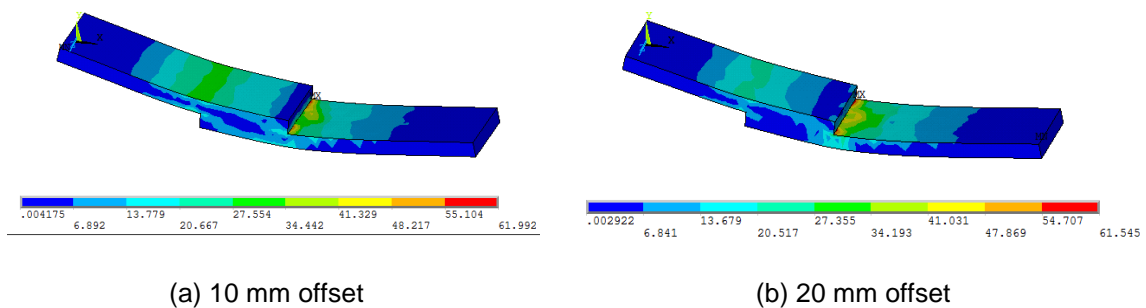


Fig. 9. Equivalent stress graphs with offset

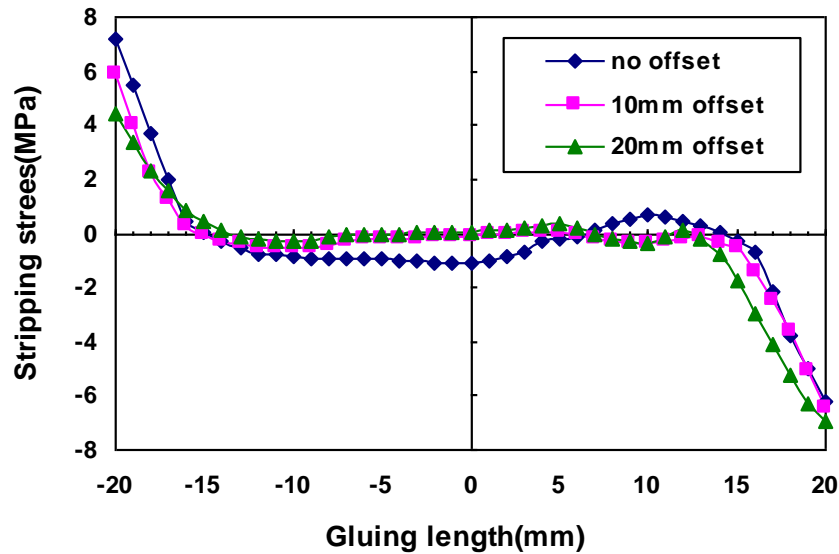


Fig. 10. Stripping stress curves for different offsets

From the above simulation analyses, it can be seen that the peak stripping stress at the left of the joint had the greatest effect on the joint's flexural performance. Finite element simulation analysis showed that the change in the peak stripping stress at the left of the joint can be examined as a function of the loading position. The left offsets of loading position were chosen as 10 mm and 20 mm, their respective equivalent stress graphs are shown in Fig. 9, and the corresponding stripping stress curves with 10 mm offset and 20 mm offset are shown in Fig. 10. The above curves show that the equivalent stress distribution changed greatly. The maximum stress area moved from the left end (which cracked more easily) to the right end, the peak stripping stress at the left end decreased with increasing offset, and the middle region of the stress curve became flatter and the values were closer to zero, so that the flexural performance of the joint increased. This shows that a carefully chosen loading position can improve the bending capacity of joints.

## CONCLUSIONS

1. From the intuitive analysis of the bending destructive test, it was seen that the values of MOE and MOR increased with an increase in sample length, but were reduced with an increase in sample thickness. The effect of sample width can be ignored.
2. The magnitudes of  $E_f$  and MOE were not consistent, but the values for each group of samples showed the same trend. The mean values of  $E_f$  and MOE generally increased with increasing length to thickness ratio and became equal at a particular length to thickness ratio. The correlations between  $E_f$  and MOE, as well as  $E_f$  and MOR were very highly significant. The FFT flexural vibration method can be used for the nondestructive testing of wood single lap glued joints.



3. Finite element simulation (FES) of wood single lap glued joints showed that the stress and deformation were symmetrical, with the peak stripping stress appearing at both ends of the joint. The peak stripping stress decreased gradually with increasing gluing length and thickness. After changing the loading position, the maximum equivalent stress area moved from the left end to the right end. The peak stripping stress decreased with increasing offset, and the flexural performance of the joint was enhanced. Thus, FES can enable optimized design of joints and provide improvement of the joint bearing position in practical applications.

## ACKNOWLEDGMENTS

This project was supported by the Fundamental Research Funds for the Central Universities (DL12EB03), National Natural Science Foundation of China (31170516, 31010103905), Excellent Doctoral Dissertation Foster Planning of Northeast Forestry (GRAD09).

## REFERENCES CITED

- Abdolahian Sohi, A. M., Khademi-Eslam, H., Hemmasi, A. H., Roohnia, M., and Talaiepour, M. (2011). "Nondestructive detection of the effect of drilling on acoustic performance of wood," *BioResources* 6(3), 2632-2646.
- Cheng, F., and Hu, Y. (2011). "Reliability analysis of timber structure design of poplar lumber with nondestructive testing methods," *BioResources* 6(3), 3188-3198.
- Cheng, K. (2005). *The Design and Analysis of Experiments*, Tsinghua University Press of China, Beijing.
- Cohen, L. (1989). "Time-frequency distributions: A review," *Proceedings of the IEEE*, 77, 941-981.
- Custodio, J., Broughton, J., and Cruz, H. (2009). "A review of factors influencing the durability of structural bonded timber joints," *Int. J. Adhes. Adhes.* 29, 173-185.
- Gu, J. (2003). *Gluing Theory and Gluing Basis*, Science Press of China, Beijing.
- Hu, Y. C. (2004). *Dynamic Properties and Nondestructive Testing of Wood-based Composites*, Northeast Forestry University Press, Harbin, China.
- Hu, Y., Wang, F., Liu, Y., and Tetsuya, N. (2001). "Study on modulus of elasticity in bending of plywood by vibration method," *China Wood Industry* 15(2), 3-5, 8.
- Li, W., Ma, C., and Shen, S. (2011). "Research progress and prospect on laminated veneer lumber," *Wood Processing Machinery* 4, 35-39.
- Liu, Z., Shen, J., Liu, Y., Liu, M., Zhang, H., and Shang, J. (2007). "Acoustic vibration property of full-size spruce wood soundboard of musical instruments," *Scientia Silvae Sinicae* 43, 100-105.
- Liu, Z., and Ta, D. (2000). "Mode identify of Lamb wave by means of 2-D FFT," *Technical Acoustics* 19, 212-219.
- Prosser, W., Seale, M. D., Smith, B. T. (1999). "Time-frequency analysis of the dispersion of Lamb modes," *J. Acoust. Soc. Am.* 105, 2669-2676.
- Rokhlin, S., and Marom, D. (1986). "Study of adhesive bonds using low-frequency obliquely incident ultrasonic waves," *J. Acoust. Soc. Am.* 80, 585-590.

- Ta, D., and Liu, Z. (2001). "Application of two-dimensional signal analysis in ultrasonic nondestructive testing," *Applied Acoustics* 20, 40-44.
- Ye, K. (1989). "A study on the relationship between the tensile strength and the thickness structure in plywood," *Wood Industry* 3, 13-19.
- Yoshihara, H. (2012). "Influence of the specimen depth to length ratio and lamination construction on Young's modulus and in-plane shear modulus of plywood measured by flexural vibration," *BioResources* 7(1), 1337-1351.

Article submitted: July 30, 2012; Peer review completed: September 4, 2012; Revised version received and accepted: September 12, 2012; Published: September 17, 2012.